

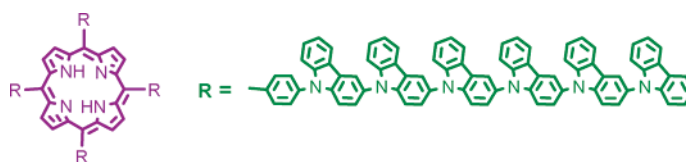
## Porphyrins with Four Monodisperse Oligocarbazole Arms: Facile Synthesis and Photophysical Properties

Tinghua Xu, Ran Lu,\* Xingliang Liu, Peng Chen, Xianping Qiu, and Yingying Zhao

State Key Laboratory of Supramolecular Structure and Materials, College of Chemistry, Jilin University, Changchun 130012, People's Republic of China

luran@mail.jlu.edu.cn

Received November 12, 2007



A series of novel monodisperse, well-defined, star-shaped molecules T(OCA $n$ )Ps ( $n = 2-6$ ) with a central porphyrin core and four oligocarbazole arms are synthesized from the corresponding formyl-substituted oligocarbazoles via Adler reaction. The obtained star-shaped porphyrins are intrinsically two-dimensional nanosized molecules, and the diameter of compound T(OCA6)P is 7.4 nm, representing one of the largest known star-shaped conjugated systems. Their photophysical properties have been investigated by absorption and steady-state fluorescence spectroscopy, together with the corresponding monodisperse oligocarbazole aldehyde precursors. It is found that the light-harvesting capability of T(OCA $n$ )Ps increases with the increasing length of the arms and reaches the maximum when  $n = 6$ . A selective excitation of the oligocarbazole arms leads to the typical emission from the porphyrin cores, indicating occurrence of photoinduced intramolecular energy transfer, and the energy transfer efficiency decreases from T(OCA2)P to T(OCA6)P owing to the Förster energy-transfer process. Accordingly, the longest effective distance for Förster energy transfer is estimated to be ca. 3 nm in our system. Such star-shaped porphyrins may find applications in photonic devices, with respect to their intense emission of red light. Notably, the monodisperse oligocarbazole aldehyde precursors give twisted intramolecular charge-transfer (TICT) excited states and luminescence in polar solvents with large Stokes shifts.

### Introduction

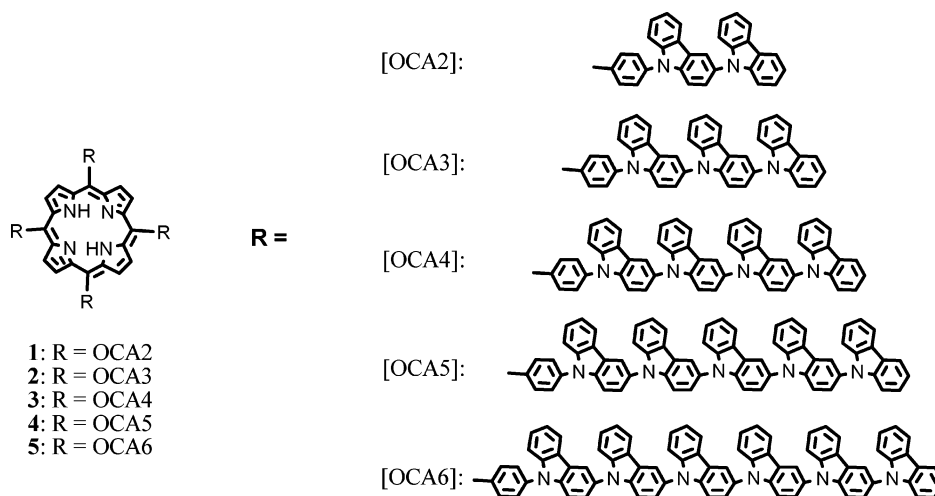
Star-shaped molecules, in which linear arms are joined together by a central core, have received much attention in the past decade,<sup>1</sup> specially the star-shaped architecture with conjugated moieties as the arms would exhibit novel electrical, optical, and morphological properties, depending on the structure of the central core. Nowadays, monodisperse linear  $\pi$ -conjugated oligomers (MCOs) bearing well-defined and uniform structures are of great interest in materials science,<sup>2</sup> due to their potential applications in organic light emitting diodes,<sup>3</sup> field effect transistors,<sup>4</sup> photovoltaic cells,<sup>5</sup> and molecular wires in the fields of molecular electronics as well as in light-harvesting molecular antenna-type architecture.<sup>6</sup> Moreover, MCOs not only become ideal models for understanding the structure–property relationships of the corresponding conjugated polymers, but also favor

tuning the electronic structures as well as the bandgaps of the oligomers.<sup>2,7,8</sup> Therefore, the monodisperse conjugated star-shaped systems, on one hand, may become possible alternatives to linear conjugated oligomers in optoelectronic applications.<sup>9</sup> On the other hand, the communication between the conjugated arms and core may result in some unique functionality.<sup>10</sup>

Because of the outstanding photophysical and redox properties porphyrins have been recently widely used as building blocks in the construction of  $\pi$ -conjugated molecules, possessing potential applications in molecular electronics, photochemical energy conversion and storage, switches, etc.<sup>6a,10,11</sup> As reported by Bo and co-workers, porphyrin was employed as the core to

(1) (a) Moore, J. S. *Acc. Chem. Res.* **1997**, *30*, 402–413. (b) Hadjichristidis, N.; Pitsik, M.; Pispas, S.; Iatrou, H. *Chem. Rev.* **2001**, *101*, 3747–3792.

(2) (a) Tour, J. M. *Chem. Rev.* **1996**, *96*, 537–553. (b) Martin, R. E.; Diederich, F. *Angew. Chem., Int. Ed.* **1999**, *38*, 1350–1377. (c) Tour, J. M. *Acc. Chem. Res.* **2000**, *33*, 791–804. (d) Holten, D.; Bocian, D. F.; Lindsey, J. S. *Acc. Chem. Res.* **2002**, *35*, 57–69. (e) Kim, D.; Osuka, A. *Acc. Chem. Res.* **2004**, *37*, 735–745. (f) Caminade, A.-M.; Majoral, J.-P. *Acc. Chem. Res.* **2004**, *37*, 341–348. (g) Grimsdale, A. C.; Müllen, K. *Angew. Chem., Int. Ed.* **2005**, *44*, 5592–5629. (h) Schwab, P. F. H.; Smith, J. R.; Michl, J. *Chem. Rev.* **2005**, *105*, 1197–1279.

SCHEME 1. Molecular Structures of T(OCA $n$ )Ps 1–5

construct star-shaped oligofluorenes, in which the photoinduced intramolecular energy transfer from oligofluorene arms to the core could be intensified with increased conjugated length of the oligofluorene arms.<sup>10c</sup> More recently, Meijer et al. introduced oligo(*p*-phenylene vinylene) (OPV) into the porphyrin core, and studied the energy and electron transfer in the  $\pi$ -conjugated assemblies based on OPV–Zn porphyrin, OPV–H<sub>2</sub> porphyrin, and C<sub>60</sub>.<sup>10e,i</sup> Such model systems not only contribute to our understanding of photosynthesis, but also provide an entry to molecular electronics and molecular optics, which could enable us to realize transport of information on a molecular level by ultrafast energy- and electron-transfer processes, which highly depend on the morphology of molecules.<sup>6a,12</sup> Furthermore, carbazoles are also alluring molecules on account of their special photoelectric properties, for instance, the intense luminescence

favoring them to be used in OLEDs as blue emitters, and the facile oxidation processes making them suitable as hole carriers.<sup>13</sup> In addition, carbazole can be readily functionalized at 3-, 6-, or 9-positions and covalently linked to other molecular moieties,<sup>11h,14–15</sup> which prompted us to prepare a series of monodisperse oligocarbazoles linked via 3,9-positions (OCA $n$ s).<sup>15a</sup> To the best of our knowledge, there is no report on the star-shaped molecules with monodisperse oligocarbazoles as the arms. Herein, we present the strategy toward novel nanosized star-shaped porphyrins T(OCA $n$ )Ps 1–5 incorporating OCA $n$ s as arms (as shown in Scheme 1). In the case of compound 5, its molecular diameter reaches 7.4 nm, representing one of the largest known star-shaped conjugated systems. In addition, the photophysical investigation reveals that efficient photoinduced intramolecular energy transfer occurs from OCA $n$ s arms to the porphyrin core, and the energy transfer efficiency decreases with the increasing length of the oligocarbazole arms. The obtained porphyrins can emit intense red light. So these functionalized porphyrins may find applications in optical devices.

## Results and Discussion

**Syntheses of OCA $n$ -CHO 6–10.** The formyl-substituted oligocarbazoles 6–10 have been synthesized via Ullmann condensation reaction between *p*-iodobenzaldehyde and 3,9-linked monodisperse oligocarbazoles 13, 15, 17, 19, and 21, whose synthetic routes are shown in Scheme 2. 3-Iodo-9-tosylcarbazole 11, as a key compound to prolong the length of the oligocarbazoles, was prepared according to the literature.<sup>16</sup> The Ullmann condensation reaction between compound 11 and carbazole, which was catalyzed by Cu<sub>2</sub>O in *N,N*-dimethylacetamide (DMAc) at 160 °C for 24 h, gave 12 in a yield of

(3) Van Hutten, P. F.; Wideman, J.; Meetsma, A.; Hadziioannou, G. *J. Am. Chem. Soc.* **1999**, *121*, 5910–5918.

(4) (a) Garnier, F.; Yassar, A.; Hajlaoui, R.; Horowitz, G.; Deloffre, F.; Servet, B.; Ries, S.; Alnot, P. *J. Am. Chem. Soc.* **1993**, *115*, 8716–8721. (b) Katz, H. E. *J. Mater. Chem.* **1997**, *7*, 369–376. (c) Schon, J. H.; Dodabalapur, A.; Kloc, C.; Batlogg, B. *Science* **2000**, *290*, 963–965.

(5) (a) Eckert, J. F.; Nicoud, J. F.; Nierengarten, J. F.; Liu, S.; Echegoyen, L.; Barigelletti, F.; Armaroli, N.; Ouali, L.; Krasnikov, V.; Hadziioannou, G. *J. Am. Chem. Soc.* **2000**, *122*, 7467–7479. (b) de la Cruz, J. L. D.; Hahn, U.; Nierengarten, J. F. *Tetrahedron Lett.* **2006**, *47*, 3715–3718.

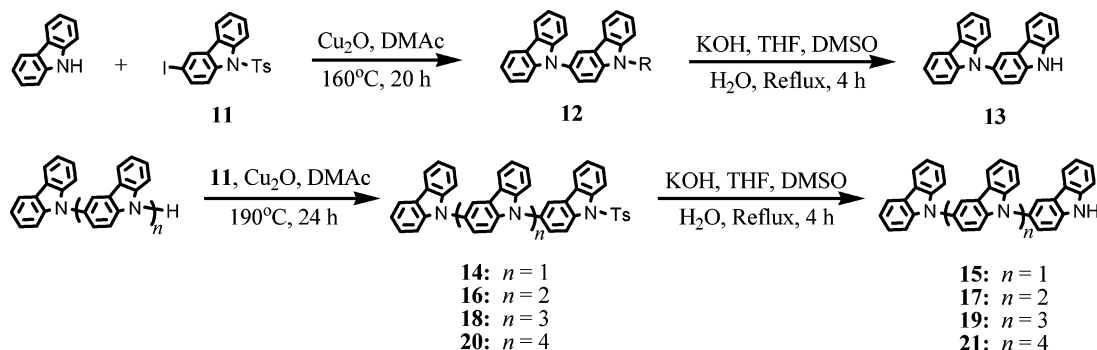
(6) (a) Wasielewski, M. R. *Chem. Rev.* **1992**, *92*, 435–461. (b) Imahori, H.; Sakata, Y. *Adv. Mater.* **1997**, *9*, 537–546. (c) Martín, N.; Sánchez, L.; Illescas, B.; Pérez, I. P. *Chem. Rev.* **1998**, *98*, 2527–2547. (d) Imahori, H.; Sakata, Y. *Eur. J. Org. Chem.* **1999**, 2445–2457.

(7) (a) Roncali, J. *Acc. Chem. Res.* **2000**, *33*, 147–156. (b) Nielsen, M. B.; Diederich, F. *Chem. Rev.* **2005**, *105*, 1837–1867.

(8) (a) Tour, J. M.; Wu, R. *Macromolecules* **1992**, *25*, 1901–1907. (b) Louie, J.; Hartwig, J. F. *Macromolecules* **1998**, *31*, 6737–6739. (c) Anderson, H. L. *Chem. Commun.* **1999**, 2323–2330. (d) Read, M. W.; Escobedo, J. O.; Willis, D. M.; Beck, P. A.; Strogan, R. M. *Org. Lett.* **2000**, *2*, 3201–3204. (e) Robert, F.; Winum, J. Y.; Sakai, N.; Gerard, D.; Matile, S. *Org. Lett.* **2000**, *2*, 37–39. (f) Fujii, K.; Furuta, T.; Tanaka, K. *Org. Lett.* **2001**, *3*, 169–171. (g) Anémian, R.; Mulatier, J. C.; Andraud, C.; Stéphan, O.; Vial, J. C. *Chem. Commun.* **2002**, 1608–1609. (h) Geng, Y.; Trajkovska, A.; Katsis, D.; Ou, J.; Culligan, S. W.; Chen, S. H. *J. Am. Chem. Soc.* **2002**, *124*, 8337–8347. (i) Aratani, N.; Cho, H. S.; Ahn, T. K.; Cho, S.; Kim, D.; Sumi, H.; Osuka, A. *J. Am. Chem. Soc.* **2003**, *125*, 9668–9681. (j) Jo, J. H.; Chi, C. Y.; Höger, S.; Wegner, G.; Yoon, D. Y. *Chem.-Eur. J.* **2004**, *10*, 2681–2688. (k) Li, J.; Li, M.; Bo, Z. *Chem.-Eur. J.* **2005**, *11*, 6930–6936. (l) Narutaki, M.; Takimiya, K.; Otsubo, T.; Harima, Y.; Zhang, H.; Araki, Y.; Ito, O. *J. Org. Chem.* **2006**, *71*, 1761–1768. (m) Zhang, X.; Qu, Y.; Bu, L.; Tian, H.; Zhang, J.; Wang, L.; Geng, Y.; Wang, F. *Chem.-Eur. J.* **2007**, *13*, 6238–6248. (n) Zhao, Z.; Xu, X.; Jiang, Z.; Lu, P.; Yu, G.; Liu, Y. *J. Org. Chem.* **2007**, *72*, 8345–8353. (o) Nishide, Y.; Osuga, H.; Saito, M.; Aiba, T.; Inagaki, Y.; Doge, Y.; Tanaka, K. *J. Org. Chem.* **2007**, *72*, 9141–9151.

(9) (a) Cherioux, F.; Guyard, L. *Adv. Funct. Mater.* **2001**, *11*, 305–309. (b) de Bettignies, R.; Nicolas, Y.; Blanchard, P.; Levillain, E.; Nunzi, J.-M.; Roncali, J. *Adv. Mater.* **2003**, *15*, 1939–1943. (c) Ponomarenko, S. A.; Kirchmeyer, S.; Elschner, A.; Huisman, B.-H.; Karbach, A.; Drechsler, D. *Adv. Funct. Mater.* **2003**, *13*, 591–596. (d) Zhou, X.-H.; Yan, J.-C.; Pei, J. *Org. Lett.* **2003**, *5*, 3543–3546. (e) Pei, J.; Wang, J.-L.; Cao, X.-Y.; Zhou, X.-H.; Zhang, W.-B. *J. Am. Chem. Soc.* **2003**, *125*, 9944–9945. (f) Kanibolotsky, A. L.; Berridge, R.; Skabara, P. J.; Perepichka, I. F.; Bradley, D. D. C.; Koeberg, M. *J. Am. Chem. Soc.* **2004**, *126*, 13695–13702. (g) Sun, Y.; Xiao, K.; Liu, Y.; Wang, J.; Pei, J.; Yu, G.; Zhu, D. *Adv. Funct. Mater.* **2005**, *15*, 818–822. (h) Wang, J.-L.; Duan, X.-F.; Jiang, B.; Gan, L.-B.; Pei, J.; He, C.; Li, Y.-F. *J. Org. Chem.* **2006**, *71*, 4400–4410. (i) Omer, K. M.; Kanibolotsky, A. L.; Skabara, P. J.; Perepichka, I. F.; Bard, A. J. *J. Phys. Chem. B* **2007**, *111*, 6612–6619.

## SCHEME 2. Syntheses of Compounds 13, 15, 17, 19, and 21



83%.<sup>11h,14c–f,15</sup> Compound **13** was readily obtained by cleaving N–Ts bond of compound **12** in the mixture of THF/DMSO (2/1, v/v), H<sub>2</sub>O, and KOH under reflux for 3–4 h in a high yield of 95%. As reported, the reactivity of the N–H bond in the carbazole under the Ullmann condensation reaction decreased with the increasing number of carbazole units in OCAn<sub>s</sub>.<sup>14c–f,15</sup> Therefore, the Ullmann reactions between compound **11** and dicarbazole **13** were carried out at higher temperature (190 °C) for 24 h to afford compound **14** in a yield

of 80%, followed by the cleavage of N–Ts bond under the basic environment to give compound **15**. By using alternative Ullmann condensation and basic hydrolysis reactions, compounds **17**, **19**, and **21** were obtained in yields of ca. 69% for two steps. Subsequently, the monodisperse oligocarbazole aldehydes (OCAn–CHO) **6–10** could be easily synthesized from dicarbazole **13**, tricarbazole **15**, tetracarbazole **17**, pentacarbazole **19**, and hexacarbazole **21** via Ullmann condensation reaction with *p*-iodobenzaldehyde, and the synthetic routes were shown in Scheme 3. We have previously found that the aldehyde group could be partially oxidized by Cu<sub>2</sub>O at higher temperature under the Ullmann condensation condition, for example, it was oxidized completely over 190 °C for 24 h.<sup>15d</sup> However, we succeeded in preparing the formyl-substituted oligocarbazoles **6–10** at lower temperature (165–170 °C) for 18 h in yields of 65–81%. As mentioned above, the Ullmann condensation reactions between 3-iodo-9-tosylcarbazole and compounds **13**, **15**, **17**, **19**, and **21** were carried out at 190 °C for 24 h due to the lower reactivity of oligocarbazoles. Concerned with the higher reactivity of *p*-iodobenzaldehyde than 3-iodo-9-tosylcarbazole owing to the electron-pulling effect of the aldehyde group, the reaction between *p*-iodobenzaldehyde and oligocarbazoles was carried out at lower temperature to avoid the oxidation of the aldehydes.

**Syntheses of T(OCAn)Ps (n = 2–6).** The syntheses of the star-shaped porphyrins with monodisperse oligocarbazole arms T(OCAn)Ps were shown in Scheme 4. The obtained aldehydes **6–10** were converted into the corresponding porphyrins T(OCAn)Ps **1–5** under the modified Adler–Longo reaction condition in xylene by using *p*-nitrobenzoic acid as the catalyst in yields of 18%, 20%, 25%, 23%, and 26%, respectively.<sup>15b,17</sup> The yields were higher than those of dendritic carbazole-based porphyrins previously reported by our group<sup>15b</sup> because of the less sterically hindered effect of the carbazole aldehydes **6–10** than that of the dendritic ones. The reaction time was prolonged from 6 to 48 h for the preparation of compounds **1–5** due to the decreased reactivity of formyl-substituted oligocarbazoles with increasing number of carbazole units. For instance, the formation of T(OCA2)P **1** from compounds **6** needed 6 h, while T(OCA3)P **2** and T(OCA4)P **3** were obtained over 15 and 24 h, respectively. In the case of T(OCA5)P **4** and T(OCA6)P **5**,

(15) (a) Xu, T.; Lu, R.; Jin, M.; Qiu, X.; Xue, P.; Bao, C.; Zhao, Y. *Tetrahedron Lett.* **2005**, *46*, 6883–6886. (b) Xu, T.; Lu, R.; Qiu, X.; Liu, X.; Xue, P.; Tan, C.; Bao, C.; Zhao, Y. *Eur. J. Org. Chem.* **2006**, 4014–4020. (c) Xu, T.; Lu, R.; Liu, X.; Zheng, X.; Qiu, X.; Zhao, Y. *Org. Lett.* **2007**, *9*, 797–800. (d) Xu, T.; Lu, R.; Liu, X.; Chen, P.; Qiu, X.; Zhao, Y. *Eur. J. Org. Chem.*, published online Dec 12, 2007, 10.1002/ejoc.200700981.

(16) Tucker, S. H. *J. Chem. Soc.* **1926**, 546–553.

(17) Adler, A. D.; Longo, F. R.; Finarelli, J. D.; Goldmacher, J.; Assour, J.; Korsakoff, L. *J. Org. Chem.* **1967**, *32*, 476–476.

(10) (a) Vollmer, M. S.; Würthner, F.; Effenberger, F.; Emele, P.; Meyer, D. U.; Stimpfig, T.; Port, H.; Wolf, H. C. *Chem.-Eur. J.* **1998**, *4*, 260–269. (b) Harth, E. M.; Hecht, S.; Helms, B.; Malmstrom, E. E.; Fréchet, J. M. J.; Hawker, C. J. *J. Am. Chem. Soc.* **2002**, *124*, 3926–3938. (c) Li, B.; Li, J.; Fu, Y.; Bo, Z. *J. Am. Chem. Soc.* **2004**, *126*, 3430–3431. (d) Fei, Z.; Li, B.; Bo, Z.; Lu, R. *Org. Lett.* **2004**, *6*, 4703–4706. (e) Wolffs, M.; Hoeben, F. J. M.; Beckers, E. H. A.; Schenning, A. P. H. J.; Meijer, E. W. *J. Am. Chem. Soc.* **2005**, *127*, 13484–13485. (f) Duan, X. F.; Wang, J. L.; Pei, J. *Org. Lett.* **2005**, *7*, 4071–4074. (g) Montes, V. A.; Pérez-Bolívar, C.; Agarwal, N.; Shinar, J.; Anzenbacher, P., Jr. *J. Am. Chem. Soc.* **2006**, *128*, 12436–12438. (h) Jiu, T.; Li, Y.; Gan, H.; Li, Y.; Liu, H.; Wang, S.; Zhou, W.; Wang, C.; Li, X.; Liu, X.; Zhu, D. *Tetrahedron* **2007**, *63*, 232–240. (i) Hoeben, F. J. M.; Wolffs, M.; Zhang, J.; De Feyter, S.; Leclere, P.; Schenning, A. P. H. J.; Meijer, E. W. *J. Am. Chem. Soc.* **2007**, *129*, 9819–9828. (j) Montes, V. A.; Pérez-Bolívar, C.; Estrada, L. A.; Shinar, J.; Anzenbacher, P., Jr. *J. Am. Chem. Soc.* **2007**, *129*, 12598–12599.

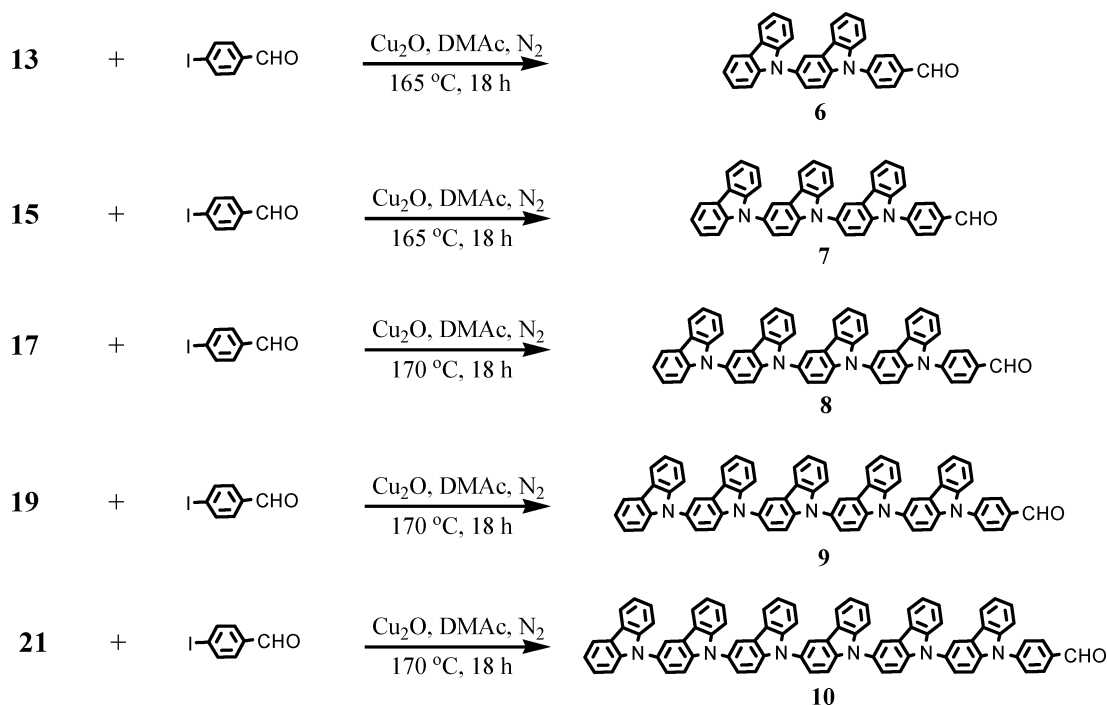
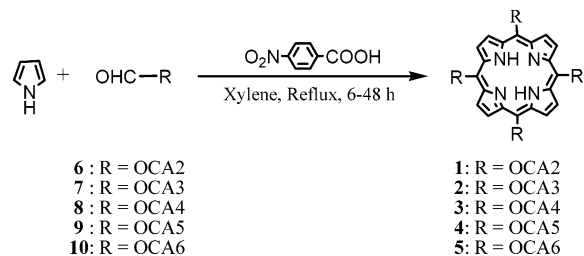
(11) (a) Gust, D.; Moore, T. A.; Moore, A. L. *Acc. Chem. Res.* **1993**, *26*, 198–205. (b) Harriman, A.; Sauvage, J. P. *Chem. Soc. Rev.* **1996**, 41–48. (c) Seth, J.; Palaniappan, V.; Wagner, R. W.; Johnson, T. E.; Lindsey, J. S.; Bocian, D. F. *J. Am. Chem. Soc.* **1996**, *118*, 11194–11207. (d) Kuciauskas, D.; Liddell, P. A.; Lin, S.; Johnson, T. E.; Weghorn, S. J.; Lindsey, J. S.; Moore, A. L.; Moore, T. A.; Gust, D. *J. Am. Chem. Soc.* **1999**, *121*, 8604–8614. (e) Ikemoto, J.; Takimiya, K.; Aso, Y.; Otsubo, T.; Fujitsuka, M.; Ito, O. *Org. Lett.* **2002**, *4*, 309–311. (f) Imaoka, T.; Horiguchi, H.; Yamamoto, K. *J. Am. Chem. Soc.* **2003**, *125*, 340–341. (g) Choi, M. S.; Yamazaki, T.; Yamazaki, I.; Aida, T. *Angew. Chem., Int. Ed.* **2004**, *43*, 150–158. (h) Loiseau, F.; Campagna, S.; Hameurlaine, A.; Dehaen, W. *J. Am. Chem. Soc.* **2005**, *127*, 11352–11363. (i) Maes, W.; Vanderhaeghen, J.; Smeets, S.; Asokan, C. V.; Van Renterghem, L. M.; Du Prez, F. E.; Smet, M.; Dehaen, W. *J. Org. Chem.* **2006**, *71*, 2987–2994. (j) Barker, C. A.; Zeng, X.; Bettington, S.; Batsanov, A. S.; Bryce, M. R.; Beeby, A. *Chem.-Eur. J.* **2007**, *13*, 6710–6717. (k) Richardson, C.; Reed, C. A. *J. Org. Chem.* **2007**, *72*, 4750–4755.

(12) Latt, S. A.; Cheung, H. T.; Blout, E. R. *J. Am. Chem. Soc.* **1965**, *87*, 995–1003.

(13) Grazulevicius, J. V.; Strohriegel, P.; Pielichowski, J.; Pielichowski, K. *Prog. Polym. Sci.* **2003**, *28*, 1297–1353.

(14) (a) Zhu, Z.; Moore, J. S. *J. Org. Chem.* **2000**, *65*, 116–123. (b) Grigalevicius, S.; Grazulevicius, J. V.; Gaidelis, V.; Jankauskas, V. *Polymer* **2002**, *43*, 2603–2608. (c) Hameurlaine, A.; Dehaen, W. *Tetrahedron Lett.* **2003**, *44*, 957–959. (d) McClenaghan, N. D.; Passalacqua, R.; Loiseau, F.; Campagna, S.; Verheyde, B.; Hameurlaine, A.; Dehaen, W. *J. Am. Chem. Soc.* **2003**, *125*, 5356–5365. (e) Kimoto, A.; Cho, J. S.; Higuchi, M.; Yamamoto, K. *Macromolecules* **2004**, *37*, 5531–5537. (f) Kimoto, A.; Cho, J.-S.; Ito, K.; Aoki, D.; Miyake, T.; Yamamoto, K. *Macromol. Rapid Commun.* **2005**, *26*, 597–601. (g) Ding, J.; Gao, J.; Cheng, Y.; Xie, Z.; Wang, L.; Ma, D.; Jing, X.; Wang, F. *Adv. Funct. Mater.* **2006**, *16*, 575–581. (h) Adhikari, R. M.; Mondal, R.; Shah, B. K.; Neckers, D. C. *J. Org. Chem.* **2007**, *72*, 4727–4732. (i) Zhao, Z.; Zhao, Y.; Lu, P.; Tian, W. *J. Phys. Chem. C* **2007**, *111*, 6883–6888.



SCHEME 3. Syntheses of OCA<sub>n</sub>-CHO 6–10SCHEME 4. Syntheses of T(OCA<sub>n</sub>)Ps 1–5

even if the reaction time was prolonged to 48 h, a small quantity of aldehyde precursors still remained. According to the previous reports, the Adler condensation conditions are harsh and the yields are low, but we obtained the functionalized porphyrins in moderate yields in this application. We have also employed the Lindsey reaction to prepare these star-shaped porphyrins, but only traces of T(OCA<sub>n</sub>)Ps were obtained with use of trifluoroacetic acid as the catalyst in CH<sub>2</sub>Cl<sub>2</sub> in the dark, followed by DDQ oxidation and Et<sub>3</sub>N neutralization.<sup>18</sup>

Notably, the obtained star-shaped porphyrins T(OCA<sub>n</sub>)Ps 1–5 bear no alkyl groups, but they are well soluble in common organic solvents, such as chloroform, CH<sub>2</sub>Cl<sub>2</sub>, chlorobenzene, toluene, xylene, mesitylene, and THF. The diameters of T(OCA<sub>n</sub>)Ps 1–5 are estimated from the optimized geometry (Cerius 2.0, Figures S49–S53) to be 3.4, 4.5, 5.4, 6.5, and 7.4 nm, respectively, and 5 represents one of the largest known star-shaped molecules. All the intermediates and final products were purified by column chromatography on silica gel, and characterized by FT-IR, <sup>1</sup>H NMR spectroscopy, C, H, and N elemental analyses, and MALDI-TOF mass spectrometry. Meanwhile, the purity of T(OCA<sub>n</sub>)Ps 1–5 was also confirmed by gel permeation chromatography (GPC) with THF as eluent. As shown in Figure 1, the retention time decreased gradually with the increasing

molecular weight from compound 1 to 5, and all the peaks were symmetrical and monomodal with a polydispersity index of 1.03–1.08. The <sup>1</sup>H NMR and the MALDI-TOF mass spectra are given in the Supporting Information.

**Photophysical Properties of OCA<sub>n</sub>-CHO 6–10.** As shown in Figure 2, the absorption spectra of OCA<sub>n</sub>-CHO 6–10 in dichloromethane exhibit intense transitions in the UV region, for instance, a broad absorption band appears at ca. 343 nm for each compound, and other broad bands in the range of 250–290 nm derive from the carbazole-centered transitions. Due to the large torsion angle of the carbazole units, no significant enlargement of the conjugation length of OCA<sub>n</sub>-CHO is observed, which is in accordance with the slight red-shift with increasing number of carbazole units. The molar extinction coefficient at 294 nm increases linearly depending on the OCA<sub>n</sub>-CHO length from dimer to hexamer, while no deviations from the slope are observed in Figure S47 (Supporting Information) (the absorption data are also listed in Table 1). It suggests that in dilute solution (1 × 10<sup>-5</sup> mol/L) neither intermolecular aggregation (according with Beer's law) nor intramolecular π–π interactions between the conjugated arms happen.<sup>19</sup> Besides the carbazole-centered transitions, the absorption band between 300 and 400 nm may also be partly contributed to the charge-transfer (CT) transitions because it is solvent dependent. Accordingly, it exhibits a tail in CH<sub>2</sub>Cl<sub>2</sub> and THF (probably due to the CT contribution), and disappears in nonpolar solvent, notably, it becomes structured in hexane (Figure S48, Supporting Information). These absorption spectral behaviors are quite similar to those of the dendritic carbazole aldehydes reported by Dehaen et al.<sup>11h</sup> Since the oligocarbazoles as strong electron-donor groups are decorated with an electron-acceptor unit (benzaldehyde) in compounds 6–10, the CT transitions could be observed in polar solvents. As it is known that dendritic carbazole aldehydes can give TICT excited state and luminescence in polar

(18) Lindsey, J. S.; Schreyman, L. C.; Hsu, H. C.; Kearney, P. C.; Marguerettaz, A. M. *J. Org. Chem.* **1987**, *52*, 827–836.

(19) Cho, S.; Li, W.-S.; Yoon, M.-C.; Ahn, T. K.; Jiang, D.-L.; Kim, J.; Aida, T.; Kim, D. *Chem.-Eur. J.* **2006**, *12*, 7576–7584.

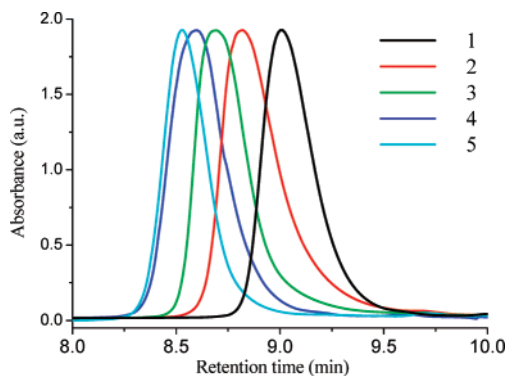


FIGURE 1. GPC elution traces of 1–5 with THF as eluent.

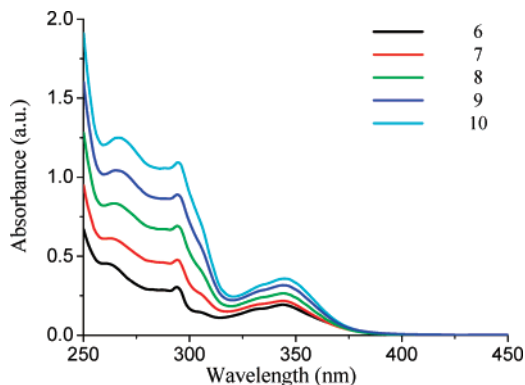


FIGURE 2. Absorption spectra of  $OCA_n$ -CHO 6–10 in  $CH_2Cl_2$  ( $1 \times 10^{-5}$  mol/L).

TABLE 1. Absorption and Fluorescent Emission Data in  $CH_2Cl_2$  for  $OCA_n$ -CHO 6–10

compd	$\lambda_{\max}^{\text{abs}}$ (nm) ( $\epsilon$ , $M^{-1} \text{ cm}^{-1}$ )	$\lambda_{\max}^{\text{em}}$ (nm)	Stokes shift (nm)
6	261 (45400), 294 (30500), 344 (19300)	525	181
7	263 (61300), 294 (47800), 344 (21800)	524	180
8	264 (83400), 294 (69200), 345 (26500)	523	178
9	265 (104300), 294 (89000), 344 (31700)	523	179
10	267 (125000), 294 (109200), 345 (35800)	524	179

solvents,<sup>11h</sup> so TICT emission of  $OCA_n$ -CHO 6–10 could be expected, which is further proposed by the following evidence: (i) the large Stokes's shift (Table 1), which rules out a singlet  $\pi$ – $\pi^*$  emission, and (ii) the broad shape of the emission spectra (Figure 3). In particular, the solvent dependence of the emission can also support the large polar character of the emitting excited state, which is in good agreement with the TICT assignment. Taking compound 6 as an example, as shown in Figure 4 we observe significant red-shift of the emission band from 385 nm in hexane to 550 nm in DMSO with increasing the solvent polarity. The emission spectrum becomes structured in hexane, similar to that of the carbazole-centered compound, so it is deemed that the excited state contributive to the emission in hexane is the LE (locally excited) one. It is well-known that the TICT state is very unlikely in nonpolar solvent, where it can hardly be stabilized.<sup>11h,20</sup> To demonstrate the large conformational change (as in the TICT formation) on the excited state surface prior to the emission, we present the plotting of the

(20) (a) Jones, G., II; Jackson, W. R.; Choi, C.; Bergmark, W. R. *J. Phys. Chem.* **1985**, *89*, 294–300. (b) Nad, S.; Pal, H. *J. Phys. Chem. A* **2001**, *105*, 1097–1106.

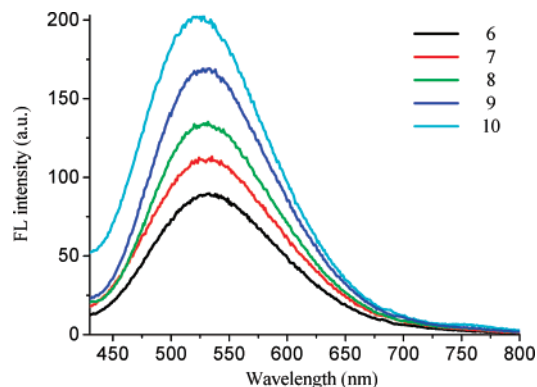


FIGURE 3. Room temperature emission spectra of the  $OCA_n$ -CHO 6–10 in  $CH_2Cl_2$  ( $1 \times 10^{-5}$  mol/L).

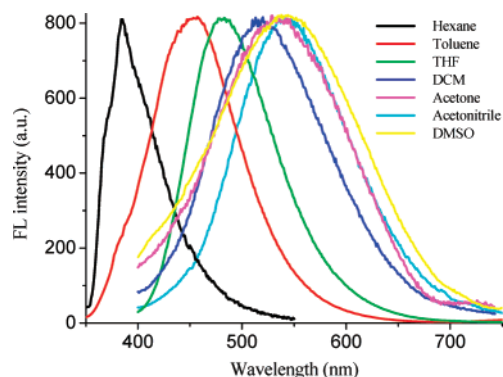


FIGURE 4. Room temperature normalized emission spectra of  $OCA_2$ -CHO 6 in solvents with different polarities.

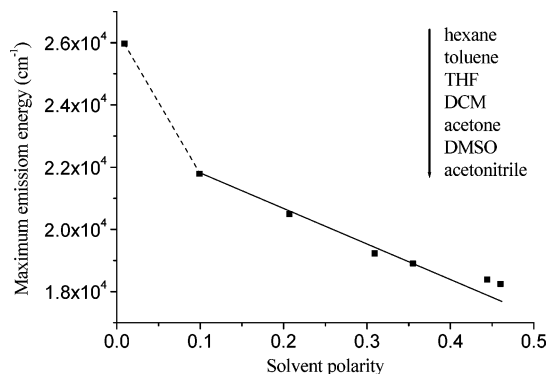


FIGURE 5. Lippert–Mataga plot: fluorescence emission maximum energy of  $OCA_2$ -CHO 6 as a function of solvent polarity.

emission maximum energy as a function of the Lippert solvent polarity in Figure 5.<sup>21</sup> In such “Lippert–Mataga” plots,<sup>11h,22</sup> the slope can be used to evaluate the variation in dipole moment upon excitation, and the break in the linear relationship indicates the presence of two different excited states. Accordingly, the deviation of the emission maximum energy in hexane from the linear relationship followed by the emission energy in other solvents can further support that in compounds 6–10 the LE state is responsible for the emission in nonpolar solvents and the TICT state is contributive to the emission in polar solvents.

(21) Reichardt, C. *Chem. Rev.* **1994**, *94*, 2319–2358.

(22) Mataga, N.; Kubota, T. *Molecular Interactions and Electronic Spectra*; Dekker: New York, 1970.

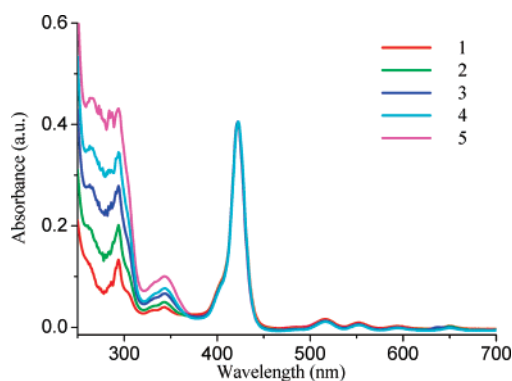


FIGURE 6. Normalized UV/vis absorption spectra of **1–5** in THF.

TABLE 2. Photophysical Data for TPP and T(OCA*n*)Ps **1–5** in THF

compd	$\lambda_{\text{max}}^{\text{abs}}$ (nm)	$\lambda_{\text{max}}^{\text{em}}$ (nm) <sup>a</sup>	$\Phi_{\text{ET}}^b$ (%)	$\Phi_{\text{F}}^c$
TPP	416	651, 717		0.110
T(OCA2)P	294, 343, 423	655, 720	100	0.173
T(OCA3)P	294, 343, 423	655, 722	100	0.170
T(OCA4)P	294, 344, 423	656, 721	95	0.167
T(OCA5)P	294, 344, 423	655, 720	90	0.157
T(OCA6)P	294, 345, 423	654, 721	76	0.145

<sup>a</sup> Excited at 294 nm. <sup>b</sup> Energy transfer efficiency ( $\Phi_{\text{ET}}$ ) was calculated by comparing the absorption with the excitation spectra of star-shaped porphyrins by monitoring the emission of the porphyrin core (655 nm). <sup>c</sup> The fluorescence quantum yields were determined against TPP in THF ( $\Phi_{\text{F}} = 0.110$ ,  $\lambda_{\text{ex}} = 423$  nm) as the standard.

**Photophysical Properties of T(OCA*n*)Ps **1–5**.** The photophysical data for T(OCA*n*)Ps **1–5** are listed in Table 2. Figure 6 shows the absorption spectra of compounds **1–5** in THF; we observe several absorption bands in visible region, including four Q-bands in the range of 500–700 nm (consistent with the free-base porphyrin), together with the Soret band at 423 nm, and others in the UV region (250–350 nm) due to the carbazole units. With the increasing length of the arms in these star-shaped molecules, the absorbance of carbazole units is clearly proportional to their increased number in each molecule, which indirectly reflects the structural flawlessness or perfection of the as-synthesized star-shaped porphyrins. Meanwhile, neither distinct spectral shift nor spectral broadening of the absorption bands for carbazole units as well as the porphyrin core is observed. Thus, it provides an opportunity to study the intramolecular energy transfer properties by selectively exciting the oligocarbazole arms, whose emission band overlaps the absorption band of the porphyrin core. As shown in Figure 7, on excitation at 294 nm, T(OCA*n*)Ps **1–5** give strong emission bands at ca. 655 and 720 nm attributable to the emission of porphyrin cores, and weak emissions at ca. 430 nm to the OCA*n*s. Since the porphyrin cannot emit red light under excitation at 294 nm, we conclude that intramolecular energy transfer from oligocarbazole units to porphyrin cores (energy trap) occurs. The light-harvesting ability is improved from **1** to **5** on account of multiplying the number of carbazole units (energy-collecting sites) and reaches the maximum when  $n = 6$ , whereas the emission intensity of T(OCA*n*)Ps **1–5** is enhanced with the increasing length of OCA*n*s arms except for compound **5**. The lower emission intensity of compound **5** than **4** might depend on its lower efficiency of energy transfer and lower fluorescence quantum yield, which will be discussed below. The energy transfer efficiency ( $\Phi_{\text{ET}}$ ) can be estimated by comparing the UV/vis spectrum with the excitation spectrum

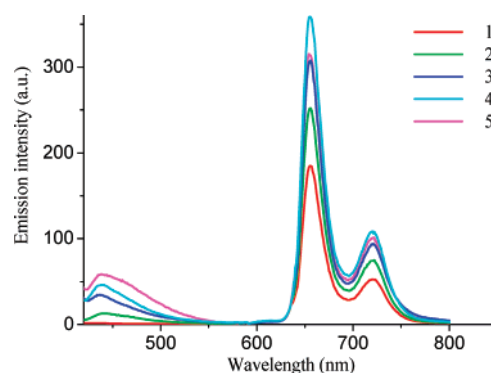


FIGURE 7. Emission spectra of T(OCA*n*)Ps **1–5** in THF ( $1 \times 10^{-6}$  mol/L,  $\lambda_{\text{ex}} = 294$  nm).

recorded at 294 nm, and the  $\Phi_{\text{ET}}$  values for T(OCA*n*)Ps **1–5** are found to be 100%, 100%, 95%, 90%, and 76%, respectively (Table 2).<sup>23</sup> The effective number of carbazoles which can transfer the light-harvesting energy to the porphyrin core in each oligocarbazole arm of compounds **1–5** is calculated as 2.0, 3.0, 3.8, 4.5, and 4.6 (the value is obtained from the multiplication between the number of carbazoles in each arm and  $\Phi_{\text{ET}}$ ), respectively. The observation that the energy-transfer efficiency decreases with the increasing length of carbazole arms can be explained by the Förster mechanism of energy transfer, and the distance between the donor and the acceptor plays an important role in the energy transfer. Generally, the Förster energy transfer may occur when the distance between energy donor and acceptor is in the range of 10–100 Å, and such resonance energy transfer depends on  $1/R^6$ , where  $R$  is the distance of the donor–acceptor separation.<sup>12</sup> As the size of star-shaped molecules increases, two competing factors, including the increasing number of carbazole units and the distance between the core and the end-groups, become prevalent. In another words, the enlargement of the molecular length allows for higher light-harvesting due to more light-collecting sites; however, to some extent, it is expected that  $R$  will become too large to sustain the energy transfer efficiency. It is thus necessary to reach a balance between the light-harvesting capacity of OCA*n*s arms and the energy transfer efficiency to the core. The distances between the outermost carbazole and the center of the porphyrin core are obtained by Cerius 2.0 to be 1.5, 2.0, 2.4, 3.0, and 3.5 nm, respectively (Figures S49–S53).<sup>24</sup> As demonstrated in the context, it is estimated that the longest distance for Förster energy transfer is ca. 3 nm in T(OCA*n*)Ps **1–5**. The emission spectra of T(OCA*n*)Ps **1–5** reveal that these star-shaped molecules can emit intense red light (Figure 7), and the fluorescence quantum yields ( $\Phi_{\text{F}}$ ) of **1–5** in THF are determined by using TPP ( $\Phi_{\text{F}} = 0.11$ ) as the standard. The  $\Phi_{\text{F}}$  values of **1–5** are in the range of 0.145–0.173 (Table 2), higher than that of TPP. Since the light energy absorbed by OCA*n*s arms can be transferred to the porphyrin core, the emission intensity ( $\lambda_{\text{ex}} = 294$  nm) of the porphyrin core is correlated to the effective carbazole number in energy transfer and the  $\Phi_{\text{F}}$  of the star-shaped molecules. The relative emission intensity for **1–5** is estimated as 1:1.4:1.8:2.1:1.9, which is the ratio of the values from the effective carbazole

(23) (a) Stryer, L.; Haugland, R. P. *Proc. Natl. Acad. Sci. U.S.A.* **1967**, *58*, 719–726. (b) Devadoss, C.; Bharathi, P.; Moore, J. S. *J. Am. Chem. Soc.* **1996**, *118*, 9635–9644. (c) Jiang, D.-L.; Aida, T. *J. Am. Chem. Soc.* **1998**, *120*, 10895–10901.

(24) Rappé, A. K.; Casewit, C. J.; Colwell, K. S.; Goddard, W. A., III; Skiff, W. M. *J. Am. Chem. Soc.* **1992**, *114*, 10024–10035.



number multiplying  $\Phi_F$ . That is in agreement with the observation of why the emission intensity of compound **5** is lower than that of compound **4**.

## Conclusions

We have designed and synthesized five soluble monodisperse star-shaped molecules with a porphyrin central core functionalized with oligocarbazole arms T(OCA $n$ )Ps **1–5**. The diameter of compound **5** is 7.4 nm, to the best of our knowledge, which represents one of the largest known conjugated star-shaped systems. The present synthetic strategy provides a useful method for the preparation of porphyrins with various functional arms. Because the emission band of monodisperse oligocarbazoles overlaps the absorption of the porphyrin, efficient photoinduced intramolecular energy transfer occurs from oligocarbazole arms to the porphyrin core. The energy transfer efficiency decreases with increasing length of the OCA $n$ s arms, although the light-harvesting ability of T(OCA $n$ )Ps increases with increasing number of carbazole units (the light-harvesting ability reaches a maximum when  $n = 6$ ), due to Förster energy-transfer mechanism. We estimate the longest distance for Förster energy transfer is ca. 3 nm in such systems. Meanwhile, the obtained star-shaped porphyrins could emit intense red light with high fluorescence quantum yields, so they might be good candidates for photonic devices.

## Experimental Section

**9-(9-Tosyl-9H-carbazol-3-yl)-9H-carbazole (12).** Carbazole (5.0 g, 0.03 mol), 3-iodo-9-tosylcarbazole **11** (11.0 g, 0.025 mol), Cu<sub>2</sub>O (7.0 g, 0.049 mol), and DMAc (25 mL) were added sequentially into a seal-tube under nitrogen atmosphere and heated to 160 °C in an oil bath for 20 h. Then the mixture was cooled to room temperature and filtrated. The filtrate was poured into 500 mL of H<sub>2</sub>O and the mixture was stirred for 20 min. The crude product was collected by filtration and recrystallized from EtOH:THF (1:1, v/v) to give 10.0 g (83%) of a white solid, mp 173.0–175.0 °C. <sup>1</sup>H NMR (500 MHz, CDCl<sub>3</sub>)  $\delta$  8.54 (d,  $J = 8.5$  Hz, 1 H), 8.40 (d,  $J = 8.5$  Hz, 1 H), 8.18 (d,  $J = 7.5$  Hz, 2 H), 8.09 (s, 1 H), 7.89 (d,  $J = 7.5$  Hz, 1 H), 7.82 (d,  $J = 7.5$  Hz, 2 H), 7.67 (d,  $J = 9.0$  Hz, 1 H), 7.58–7.55 (t, 1 H), 7.39 (m, 5 H), 7.32–7.29 (t, 2 H), 7.21 (d,  $J = 9.0$  Hz, 2 H), 2.34 (3 H, s, –CH<sub>3</sub>) (see Figures S1 and S2, Supporting Information). Anal. Calcd for C<sub>31</sub>H<sub>22</sub>N<sub>2</sub>O<sub>2</sub>S: C 76.52, H 4.56, N 5.76. Found: C 76.44, H 4.58, N 5.90.

**9-(9H-Carbazol-3-yl)-9H-carbazole (13).** Compound **12** (9.5 g, 0.02 mol) was dissolved in THF (40 mL), DMSO (20 mL), and H<sub>2</sub>O (6 mL), then KOH (12.0 g, 0.214 mol) was added. The mixture was refluxed for 4 h (monitored by TLC). Then THF was completely removed from the mixture by distillation. Then the residuals were cooled to room temperature, neutralized by HCl, and poured into 400 mL of water to give a white solid. The crude product was purified on silica gel with petroleum ether/ethyl acetate (3:1, v/v) as eluent to afford 6.2 g (95%) of a white solid, mp: 210.0–211.0 °C. <sup>1</sup>H NMR (500 MHz, CDCl<sub>3</sub>)  $\delta$  8.25 (s, 1 H), 8.22–8.18 (m, 3 H), 8.05 (d,  $J = 6.5$  Hz, 1 H), 7.62 (s, 1 H), 7.56–7.49 (m, 3 H), 7.40 (m, 4 H), 7.29 (m, 3 H) (see Figure S3, Supporting Information). MALDI-TOF: calcd 332.4, found 331.3 (see Figure S4, Supporting Information). Anal. Calcd for C<sub>24</sub>H<sub>16</sub>N<sub>2</sub>: C 86.72, H 4.85, N 8.43. Found: C 86.75, H 4.67, N 8.49.

**4-(3-(9H-Carbazol-9-yl)-9H-carbazol-9-yl)benzaldehyde (6).** Compound **13** (3.0 g, 9.0 mmol), 4-iodobenzaldehyde (2.7 g, 12.0 mmol), Cu<sub>2</sub>O (2.5 g, 17.0 mmol), and DMAc (12 mL) were added sequentially into a seal-tube under nitrogen atmosphere and heated to 165 °C in an oil bath for 18 h. Then the mixture was cooled to room temperature and filtrated. The filtrate was poured into 300

mL of H<sub>2</sub>O and the mixture was stirred for 20 min. The crude product was collected by filtration and purified by chromatography (silica gel, petroleum ether) to give 3.2 g (81%) of a light-yellow solid, mp 142.0–144.0 °C. IR (KBr, cm<sup>-1</sup>): a strong peak at 1692.8 cm<sup>-1</sup> is the  $\nu_s$  of a C=O moiety. <sup>1</sup>H NMR (500 MHz, CDCl<sub>3</sub>)  $\delta$  10.19 (s, 1 H, –CHO), 8.33 (s, 1 H), 8.24–8.21 (dd,  $J = 5.5, 4.5$  Hz, 4 H), 8.15 (d,  $J = 8.0$  Hz, 1 H), 7.92 (d,  $J = 8.0$  Hz, 2 H), 7.72 (d,  $J = 9.0$  Hz, 1 H), 7.62–7.59 (t, 2 H), 7.55–7.52 (t, 1 H), 7.47–7.38 (m, 5 H), 7.35–7.32 (t, 2 H) (see Figures S5 and S6, Supporting Information). MALDI-TOF: calcd 436.5, found 437.1 (see Figure S7, Supporting Information). Anal. Calcd for C<sub>31</sub>H<sub>20</sub>N<sub>2</sub>O: C 85.30, H 4.62, N 6.42. Found: C 85.45, H 4.69, N 6.32.

**3-(3-(9H-Carbazol-9-yl)-9H-carbazol-9-yl)-9-tosyl-9H-carbazole (14).** By following the synthetic procedure for compound **12**, and using compound **13** (7.0 g, 21.1 mmol), 3-iodo-9-tosylcarbazole **11** (10.5 g, 23.5 mmol), Cu<sub>2</sub>O (6.0 g, 42.0 mmol), and DMAc (30 mL) as reagents, and adopting the Ullmann reaction condition at 190 °C in oil bath for 24 h, 11.0 g (80%) of compound **14** was obtained after recrystallization from EtOH:THF (1:1, v/v) as a white solid, mp 183.0–185.0 °C. <sup>1</sup>H NMR (500 MHz, CDCl<sub>3</sub>)  $\delta$  8.60 (d,  $J = 9.0$  Hz, 1 H), 8.41 (d,  $J = 8.0$  Hz, 1 H), 8.31 (s, 1 H), 8.20–8.13 (m, 4 H), 7.95 (d,  $J = 7.5$  Hz, 1 H), 7.84 (d,  $J = 8.0$  Hz, 2 H), 7.76–7.74 (m, 1 H), 7.62–7.55 (m, 3 H), 7.50–7.41 (m, 7 H), 7.35–7.29 (m, 3 H), 7.22 (d,  $J = 8.5$  Hz, 2 H), 2.34 (s, 3 H, –CH<sub>3</sub>) (See Figures S8 and S9, Supporting Information). Anal. Calcd for C<sub>43</sub>H<sub>29</sub>N<sub>3</sub>O<sub>2</sub>S: C 79.24, H 4.48, N 6.45. Found: C 79.14, H 4.53, N 6.44.

**9-(9H-Carbazol-3-yl)-3-(9H-carbazol-9-yl)-9H-carbazole (15).** By following the synthetic procedure for compound **13**, and using compound **14** (9.0 g, 13.8 mmol), KOH (10.0 g, 0.179 mol), THF (40 mL), DMSO (20 mL), and H<sub>2</sub>O (5 mL) as solvents, 6.5 g (95%) of compound **15** was obtained after chromatography (silica gel, petroleum ether/ethyl acetate = 3:1, v/v) as a white solid, mp 193.0–195.0 °C. <sup>1</sup>H NMR (500 MHz, CDCl<sub>3</sub>)  $\delta$  8.31 (s, 3 H), 8.19 (d,  $J = 7.0$  Hz, 2 H), 8.15 (d,  $J = 7.5$  Hz, 1 H), 8.10 (d,  $J = 6.5$  Hz, 1 H), 7.70–7.68 (d,  $J = 6.5$  Hz, 1 H), 7.65–7.63 (d,  $J = 7.0$  Hz, 1 H), 7.54–7.42 (m, 10 H), 7.30 (s, 4 H) (see Figure S10, Supporting Information). MALDI-TOF: calcd 497.6, found 497.8 (see Figure S11, Supporting Information). Anal. Calcd for C<sub>36</sub>H<sub>23</sub>N<sub>3</sub>: C 86.90, H 4.66, N 8.44. Found: C 86.81, H 4.70, N 8.26.

**4-(3-(3-(9H-Carbazol-9-yl)-9H-carbazol-9-yl)-9H-carbazol-9-yl)benzaldehyde (7).** By following the synthetic procedure for compound **6**, and using compound **15** (2.0 g, 4.0 mmol), 4-iodobenzaldehyde (1.4 g, 6.0 mmol), Cu<sub>2</sub>O (1.2 g, 8.3 mmol), and DMAc (8 mL) as reagents, 1.8 g (74%) of compound **7** was obtained after chromatography (silica gel, petroleum ether/ethyl acetate = 3:1, v/v) as a light-yellow solid, mp 195.0–197.0 °C. IR (KBr, cm<sup>-1</sup>): a strong peak at 1699.9 cm<sup>-1</sup> is the  $\nu_s$  of a C=O moiety. <sup>1</sup>H NMR (500 MHz, CDCl<sub>3</sub>)  $\delta$  10.17 (s, 1 H, –CHO), 8.39 (s, 1 H), 8.33 (m, 1 H), 8.23–8.15 (m, 6 H), 7.91 (d,  $J = 8.5$  Hz, 2 H), 7.50 (d,  $J = 9.0$  Hz, 1 H), 7.68–7.66 (d,  $J = 8.5$  Hz, 1 H), 7.59–7.52 (m, 4 H), 7.49–7.45 (m, 2 H), 7.43–7.38 (m, 5 H), 7.35–7.29 (m, 3 H) (see Figures S12 and S13, Supporting Information). MALDI-TOF: calcd 601.7, found 602.0 (see Figure S14, Supporting Information). Anal. Calcd for C<sub>43</sub>H<sub>27</sub>N<sub>3</sub>O: C 85.83, H 4.52, N 6.98. Found: C 85.80, H 4.57, N 7.01.

**3-(3-(3-(9H-Carbazol-9-yl)-9H-carbazol-9-yl)-9H-carbazol-9-yl)-9-tosyl-9H-carbazole (16).** By following the synthetic procedure for compound **12**, using compound **15** (10.0 g, 0.02 mol), 3-iodo-9-tosylcarbazole **11** (10.0 g, 0.022 mol), Cu<sub>2</sub>O (6.0 g, 0.042 mol), and DMAc (30 mL) as reagents, and adopting the Ullmann reaction condition at 190 °C in an oil bath for 24 h, 12.0 g (73%) of compound **16** was obtained after recrystallization from EtOH:THF (3:2, v/v) as a white solid, mp 215.0–217.0 °C. <sup>1</sup>H NMR (500 MHz, CDCl<sub>3</sub>)  $\delta$  8.62 (d,  $J = 8.5$  Hz, 1 H), 8.43–8.40 (t, 2 H), 8.32 (s, 1 H), 8.20–8.15 (m, 5 H), 7.95 (d,  $J = 7.5$  Hz, 1 H), 7.85 (d,  $J = 8.0$  Hz, 2 H), 7.78–7.76 (d,  $J = 9.0$  Hz, 1 H), 7.62–7.54

(m, 5 H), 7.51–7.42 (m, 9 H), 7.38–7.28 (m, 4 H), 7.23 (d,  $J = 8.0$  Hz, 2 H), 2.35 (s, 3 H,  $-\text{CH}_3$ ) (see Figures S15 and S16, Supporting Information). Anal. Calcd for  $\text{C}_{55}\text{H}_{36}\text{N}_4\text{O}_2\text{S}$ : C 80.86, H 4.44, N 6.86. Found: C 80.81, H 4.51, N 6.65.

**3-(3-(9H-Carbazol-9-yl)-9H-carbazol-9-yl)-9H-carbazol-3-yl)-9H-carbazole (17).** By following the synthetic procedure for compound **13**, and using compound **16** (13.0 g, 0.016 mol), KOH (10.0 g, 0.179 mol), THF (60 mL), DMSO (30 mL), and  $\text{H}_2\text{O}$  (7 mL) as reagents, 10.0 g (95%) of compound **17** was obtained after chromatography (silica gel, petroleum ether/ethyl acetate = 3:1, v/v) as a white solid, mp  $>250$  °C.  $^1\text{H}$  NMR (500 MHz,  $\text{CDCl}_3$ )  $\delta$  8.40 (s, 1 H), 8.32 (s, 3 H), 8.20–8.15 (m, 4 H), 8.11 (d,  $J = 7.0$  Hz, 1 H), 7.70 (d,  $J = 7.5$  Hz, 1 H), 7.66–7.60 (m, 4 H), 7.56–7.47 (m, 7 H), 7.43 (s, 4 H), 7.37–7.30 (m, 5 H) (see Figure S17, Supporting Information). MALDI-TOF: calcd 662.8, found 661.5 (see Figure S18, Supporting Information). Anal. Calcd for  $\text{C}_{48}\text{H}_{30}\text{N}_4$ : C 86.98, H 4.56, N 8.45. Found: C 87.02, H 4.54, N 8.42.

**4-(3-(3-(3-(9H-Carbazol-9-yl)-9H-carbazol-9-yl)-9H-carbazol-9-yl)-9H-carbazol-9-yl)benzaldehyde (8).** By following the synthetic procedure for compound **6**, using compound **17** (2.0 g, 3.0 mmol), 4-iodobenzaldehyde (1.2 g, 5.2 mmol),  $\text{Cu}_2\text{O}$  (1.0 g, 7.0 mmol), and DMAc (8 mL) as reagents, and adopting the Ullmann reaction condition at 170 °C in an oil bath for 18 h, 1.8 g (78%) of compound **8** was obtained after chromatography (silica gel, petroleum ether/ $\text{CH}_2\text{Cl}_2 = 4:1$ , v/v) as a light-yellow solid, mp  $>250$  °C. IR (KBr,  $\text{cm}^{-1}$ ): a strong peak at 1701.5  $\text{cm}^{-1}$  is the  $\nu_s$  of a C=O moiety.  $^1\text{H}$  NMR (500 MHz,  $\text{CDCl}_3$ )  $\delta$  10.17 (s, 1 H,  $-\text{CHO}$ ), 8.41 (d,  $J = 6.5$  Hz, 2 H), 8.33 (s, 1 H), 8.23–8.15 (m, 7 H), 7.91 (d,  $J = 8.0$  Hz, 2 H), 7.76 (d,  $J = 8.5$  Hz, 1 H), 7.70–7.68 (d,  $J = 8.5$  Hz, 1 H), 7.63–7.48 (m, 10 H), 7.43–7.28 (m, 9 H) (see Figures S19 and S20, Supporting Information). MALDI-TOF: calcd 766.9, found 767.1 (see Figure S21, Supporting Information). Anal. Calcd for  $\text{C}_{55}\text{H}_{34}\text{N}_4\text{O}$ : C 86.14, H 4.47, N 7.31. Found: C 86.22, H 4.40, N 7.36.

**3-(3-(3-(3-(9H-Carbazol-9-yl)-9H-carbazol-9-yl)-9H-carbazol-9-yl)-9H-carbazol-9-yl)-9-tosyl-9H-carbazole (18).** By following the synthetic procedure for compound **12**, using compound **17** (8.0 g, 0.012 mol), 3-iodo-9-tosylcarbazole **11** (6.5 g, 0.015 mol),  $\text{Cu}_2\text{O}$  (3.5 g, 0.024 mol), and DMAc (20 mL) as reagents, and adopting the Ullmann reaction condition at 190 °C in an oil bath for 24 h, 9.0 g (76%) of compound **18** was obtained after recrystallization from EtOH:THF (3:2, v/v) as a white solid, mp  $>250$  °C.  $^1\text{H}$  NMR (500 MHz,  $\text{CDCl}_3$ )  $\delta$  8.63 (d,  $J = 8.0$  Hz, 1 H), 8.42 (d,  $J = 7.0$  Hz, 3 H), 8.33 (s, 1 H), 8.20–8.15 (m, 6 H), 7.96 (d,  $J = 8.0$  Hz, 1 H), 7.86 (d,  $J = 7.5$  Hz, 2 H), 7.78 (d,  $J = 8.5$  Hz, 1 H), 7.64–7.55 (m, 7 H), 7.50–7.43 (m, 11 H), 7.37–7.30 (m, 5 H), 7.24 (d,  $J = 7.5$  Hz, 2 H), 2.35 (s, 3 H,  $-\text{CH}_3$ ) (see Figures S22 and S23, Supporting Information). Anal. Calcd for  $\text{C}_{67}\text{H}_{43}\text{N}_5\text{O}_2\text{S}$ : C 81.93, H 4.41, N 7.13. Found: C 81.95, H 4.39, N 7.23.

**9-(9-(9-(9H-Carbazol-3-yl)-9H-carbazol-3-yl)-9H-carbazol-3-yl)-3-(9H-carbazol-9-yl)-9H-carbazole (19).** By following the synthetic procedure for compound **13**, and using compound **18** (8.5 g, 8.7 mmol), KOH (5.0 g, 89.2 mmol), THF (40 mL), DMSO (20 mL), and  $\text{H}_2\text{O}$  (6 mL) as reagents, 6.5 g (90%) of compound **19** was obtained after chromatography (silica gel, petroleum ether/ethyl acetate = 3:1, v/v) as a white solid, mp  $>250$  °C.  $^1\text{H}$  NMR (500 MHz,  $\text{CDCl}_3$ )  $\delta$  8.41 (s, 2 H), 8.32 (s, 2 H), 8.29 (s, 1 H), 8.20–8.09 (m, 6 H), 7.68–7.60 (m, 7 H), 7.55–7.43 (m, 13 H), 7.35–7.30 (m, 6 H) (see Figure S24, Supporting Information). MALDI-TOF: calcd 827.3, found 826.6 (see Figure S25, Supporting Information). Anal. Calcd for  $\text{C}_{60}\text{H}_{37}\text{N}_5$ : C 87.04, H 4.50, N 8.46. Found: C 87.10, H 4.57, N 8.60.

**4-(3-(3-(3-(3-(9H-Carbazol-9-yl)-9H-carbazol-9-yl)-9H-carbazol-9-yl)-9H-carbazol-9-yl)-9H-carbazol-9-yl)benzaldehyde (9).** By following the synthetic procedure for compound **6**, using compound **19** (3.0 g, 3.6 mmol), 4-iodobenzaldehyde (1.2 g, 5.2 mmol),  $\text{Cu}_2\text{O}$  (1.0 g, 6.9 mmol), and DMAc (8 mL) as reagents, and adopting the Ullmann reaction condition at 170 °C in an oil

bath for 18 h, 2.2 g (65%) of compound **9** was obtained after chromatography (silica gel, petroleum ether/ $\text{CH}_2\text{Cl}_2 = 4:1$ , v/v) as a light-yellow solid, mp  $>250$  °C. IR (KBr,  $\text{cm}^{-1}$ ): a strong peak at 1702.0  $\text{cm}^{-1}$  is the  $\nu_s$  of a C=O moiety.  $^1\text{H}$  NMR (500 MHz,  $\text{CDCl}_3$ )  $\delta$  10.18 (s, 1 H,  $-\text{CHO}$ ), 8.42 (d,  $J = 9.5$  Hz, 3 H), 8.33 (s, 1 H), 8.23–8.15 (m, 8 H), 7.92 (d,  $J = 7.5$  Hz, 2 H), 7.77 (d,  $J = 8.0$  Hz, 1 H), 7.70–7.59 (m, 7 H), 7.56–7.50 (m, 8 H), 7.43–7.31 (m, 10 H) (see Figures S26 and S27, Supporting Information). MALDI-TOF: calcd 932.1, found 932.1 (see Figure S28, Supporting Information). Anal. Calcd for  $\text{C}_{67}\text{H}_{41}\text{N}_5\text{O}$ : C 86.34, H 4.43, N 7.51. Found: C 86.60, H 4.48, N 7.32.

**3-(3-(3-(3-(9H-Carbazol-9-yl)-9H-carbazol-9-yl)-9H-carbazol-9-yl)-9H-carbazol-9-yl)-9-(9-tosyl-9H-carbazol-6-yl)-9H-carbazole (20).** By following the synthetic procedure for compound **12**, using compound **19** (9.5 g, 11.5 mmol), 3-iodo-9-tosylcarbazole **11** (6.8 g, 15.2 mmol),  $\text{Cu}_2\text{O}$  (3.5 g, 24.3 mmol), and DMAc (30 mL) as reagents, and adopting the Ullmann reaction condition at 190 °C in an oil bath for 24 h, 10.0 g (76%) of compound **20** was obtained after recrystallization from EtOH:THF (3:2, v/v) as a white solid, mp  $>250$  °C.  $^1\text{H}$  NMR (500 MHz,  $\text{CDCl}_3$ )  $\delta$  8.62 (d,  $J = 8.5$  Hz, 1 H), 8.42 (s, 4 H), 8.33 (s, 1 H), 8.20–8.15 (m, 7 H), 7.96 (d,  $J = 7.5$  Hz, 1 H), 7.86 (d,  $J = 7.5$  Hz, 2 H), 7.77 (d,  $J = 8.0$  Hz, 1 H), 7.70–7.58 (m, 8 H), 7.56–7.43 (m, 14 H), 7.37–7.30 (m, 6 H), 7.24–7.20 (m, 2 H), 2.35 (s, 3 H,  $-\text{CH}_3$ ) (see Figures S29 and S30, Supporting Information). Anal. Calcd for  $\text{C}_{79}\text{H}_{50}\text{N}_6\text{O}_2\text{S}$ : C 82.70, H 4.39, N 7.32. Found: C 82.63, H 4.56, N 7.48.

**3-(3-(3-(3-(9H-Carbazol-9-yl)-9H-carbazol-9-yl)-9H-carbazol-9-yl)-9H-carbazol-9-yl)-9-(9H-carbazol-6-yl)-9H-carbazole (21).** By following the synthetic procedure for compound **13**, and using compound **20** (7.0 g, 6.1 mmol), KOH (6.0 g, 0.11 mol), THF (30 mL), DMSO (15 mL), and  $\text{H}_2\text{O}$  (5 mL) as reagents, 5.5 g (91%) of compound **21** was obtained after chromatography (silica gel, petroleum ether/ethyl acetate = 3:1, v/v) as a white solid, mp  $>250$  °C.  $^1\text{H}$  NMR (500 MHz,  $\text{CDCl}_3$ )  $\delta$  8.43 (s, 3 H), 8.33 (s, 3 H), 8.2–8.15 (m, 6 H), 8.12 (m, 1 H), 7.70 (m, 1 H), 7.66–7.60 (m, 8 H), 7.55–7.47 (m, 11 H), 7.43 (s, 4 H), 7.31–7.26 (m, 7 H) (see Figure S31, Supporting Information). MALDI-TOF: calcd 993.2, found 993.4 (see Figure S32, Supporting Information). Anal. Calcd for  $\text{C}_{72}\text{H}_{44}\text{N}_6$ : C 87.07, H 4.47, N 8.46. Found: C 87.03, H 4.45, N 8.35.

**4-(3-(3-(3-(3-(9H-Carbazol-9-yl)-9H-carbazol-9-yl)-9H-carbazol-9-yl)-9H-carbazol-9-yl)-9H-carbazol-9-yl)benzaldehyde (10).** By following the synthetic procedure for compound **6**, using compound **21** (4.0 g, 4.0 mmol), 4-iodobenzaldehyde (1.8 g, 7.8 mmol),  $\text{Cu}_2\text{O}$  (1.5 g, 0.01 mol), and DMAc (15 mL) as reagents, and adopting the Ullmann reaction condition at 170 °C in an oil bath for 18 h, 3.1 g (70%) of compound **10** was obtained after chromatography (silica gel, petroleum ether/ $\text{CH}_2\text{Cl}_2 = 4:1$ , v/v) as a light-yellow solid, mp  $>250$  °C. IR (KBr,  $\text{cm}^{-1}$ ): a strong peak at 1701.0  $\text{cm}^{-1}$  is the  $\nu_s$  of a C=O moiety.  $^1\text{H}$  NMR (500 MHz,  $\text{CDCl}_3$ )  $\delta$  10.18 (s, 1 H,  $-\text{CHO}$ ), 8.42 (d,  $J = 10.5$  Hz, 4 H), 8.32 (s, 1 H), 8.23–8.14 (m, 9 H), 7.91 (d,  $J = 7.5$  Hz, 2 H), 7.76 (d,  $J = 8.5$  Hz, 1 H), 7.70–7.58 (m, 9 H), 7.56–7.49 (m, 10 H), 7.43–7.29 (m, 11 H) (see Figures S33 and S34, Supporting Information). MALDI-TOF: calcd 1097.3, found 1097.0 (see Figure S35, Supporting Information). Anal. Calcd for  $\text{C}_{75}\text{H}_{48}\text{N}_6\text{O}$ : C 86.47, H 4.41, N 7.66. Found: C 86.41, H 4.23, N 7.59.

**T(OCA2)P (1).** Compound **6** (0.8 g, 1.8 mmol) and *p*-nitrobenzoic acid (0.16 g, 0.1 mmol) were dissolved in xylene (40 mL). The mixture was heated to reflux, a solution of pyrrole (0.13 mL, 1.9 mmol) in xylene (5 mL) was slowly added, and the system was stirred for another 6 h. Xylene (30 mL) was distilled from the mixture, then MeOH (70 mL) was added. The crude product was collected by filtration and purified through a short pad of silica gel with  $\text{CH}_2\text{Cl}_2$  as eluent to afford the crude porphyrin. Further chromatography (silica gel, petroleum ether/ $\text{CH}_2\text{Cl}_2 = 4:3$ , v/v) gave the product as a purple solid (160 mg, 18%), mp  $>250$  °C.  $^1\text{H}$  NMR (500 MHz,  $\text{CDCl}_3$ )  $\delta$  9.22 (s, 6 H), 9.01 (d,  $J = 8.5$  Hz, 1



(H), 8.88 (s, 1 H), 8.64 (d,  $J = 8.0$  Hz, 6 H), 8.45 (s, 4 H), 8.30–8.24 (m, 12 H), 8.20–8.17 (d,  $J = 8.0$  Hz, 8 H), 8.10–8.08 (d,  $J = 8.5$  Hz, 4 H), 7.97–7.95 (d,  $J = 8.5$  Hz, 4 H), 7.78–7.76 (d,  $J = 10.0$  Hz, 4 H), 7.71–7.68 (m, 4 H), 7.54–7.49 (m, 20 H), 7.38–7.35 (m, 10 H), –2.50 (s, 2 H, –NH) (see Figure S36, Supporting Information). MALDI-TOF: calcd 1936.3, found 1936.9 (see Figure S37, Supporting Information). Anal. Calcd for  $C_{140}H_{86}N_{12}$ : C 86.84, H 4.48, N 8.68. Found: C 86.90, H 4.52, N 8.39.

**T(OCA3)P (2).** Following a procedure for the preparation of compound **1**, compound **7** (1.0 g, 1.7 mmol), *p*-nitrobenzoic acid (0.15 g, 0.9 mmol), pyrrole (0.13 mL, 1.9 mmol), and xylene (35 mL) were refluxed for 15 h to give the crude porphyrin, which was purified by column chromatography (silica gel, petroleum ether/ $CH_2Cl_2 = 1:1$  v/v) to afford compound **2** as a purple solid (220 mg, 20%), mp >250 °C.  $^1H$  NMR (500 MHz,  $CDCl_3$ )  $\delta$  9.24 (s, 6 H), 9.03 (d, 1 H), 8.90 (s, 1 H), 8.67 (d,  $J = 8.0$  Hz, 6 H), 8.54 (s, 4 H), 8.39 (s, 4 H), 8.33 (d,  $J = 7.5$  Hz, 4 H), 8.24–8.20 (m, 18 H), 8.14 (d,  $J = 9.0$  Hz, 4 H), 7.98 (d,  $J = 8.5$  Hz, 4 H), 7.85 (d,  $J = 8.5$  Hz, 4 H), 7.71 (d,  $J = 8.5$  Hz, 8 H), 7.63–7.28 (m, 48 H), –2.49 (s, 2 H, –NH) (see Figure S38, Supporting Information). MALDI-TOF: calcd 2597.0, found 2597.1 (see Figure S39, Supporting Information). Anal. Calcd for  $C_{188}H_{114}N_{16}$ : C 86.95, H 4.42, N 8.63. Found: C 86.87, H 4.43, N 8.56.

**T(OCA4)P (3).** Following a procedure for the preparation of compound **2**, compound **8** (0.93 g, 1.2 mmol), *p*-nitrobenzoic acid (0.13 g, 0.8 mmol), pyrrole (0.1 mL, 1.4 mmol), and xylene (35 mL) were refluxed for 24 h to give the crude porphyrin, which was purified by column chromatography (silica gel, petroleum ether/ $CH_2Cl_2 = 1:1$  v/v) to afford compound **3** as a purple solid (250 mg, 25%), mp >250 °C.  $^1H$  NMR (500 MHz,  $CDCl_3$ )  $\delta$  9.21 (s, 4 H), 9.02 (s, 2 H), 8.88 (s, 2 H), 8.65 (d,  $J = 7.5$  Hz, 4 H), 8.53 (s, 4 H), 8.44 (s, 6 H), 8.33 (m, 8 H), 8.26–8.12 (m, 24 H), 8.03–7.95 (m, 4 H), 7.84 (m, 4 H), 7.73–7.29 (m, 78 H), –2.51 (s, 2 H, –NH) (see Figure S40, Supporting Information). MALDI-TOF: calcd 3257.8, found 3256.7 (see Figure S41, Supporting Information). Anal. Calcd for  $C_{236}H_{142}N_{20}$ : C 87.01, H 4.39, N 8.60. Found: C 86.96, H 4.35, N 8.67.

**T(OCA5)P (4).** Compound **9** (1.1 g, 1.2 mmol) and *p*-nitrobenzoic acid (0.13 g, 0.8 mmol) were dissolved in xylene (50 mL). The mixture was heated to reflux, a solution of pyrrole (0.10 mL, 1.4 mmol) in xylene (5 mL) was slowly added, and the system was stirred for another 24 h. Then pyrrole (0.05 mL, 0.7 mmol) in

xylene (5 mL) was added, and the system was stirred for 24 h. Xylene (40 mL) was distilled from the mixture, then MeOH (70 mL) was added. The crude product was collected by filtration and purified through a short pad of silica gel with  $CH_2Cl_2$  as eluent to afford the crude porphyrin. Further chromatography (silica gel, petroleum ether/ $CH_2Cl_2 = 2:3$ , v/v) gave the product as a purple solid (270 mg, 23%), mp >250 °C.  $^1H$  NMR (500 MHz,  $CDCl_3$ )  $\delta$  9.21 (s, 4 H), 9.01 (d, 2 H), 8.88 (s, 2 H), 8.65 (d,  $J = 7.0$  Hz, 6 H), 8.53 (s, 4 H), 8.45–8.40 (m, 10 H), 8.32 (s, 8 H), 8.25–8.12 (m, 30 H), 7.96 (d,  $J = 8.0$  Hz, 4 H), 7.84 (d,  $J = 8.0$  Hz, 4 H), 7.75–7.28 (m, 94 H), –2.51 (s, 2 H, –NH) (see Figure S42, Supporting Information). MALDI-TOF: calcd 3915.4, found 3915.9 (see Figure S43, Supporting Information). Anal. Calcd for  $C_{284}H_{170}N_{24}$ : C 87.05, H 4.37, N 8.58. Found: C 87.11, H 4.29, N 8.62.

**T(OCA6)P (5).** By following a procedure for the preparation of compound **4**, and using compound **10** (1.5 g, 1.4 mmol), *p*-nitrobenzoic acid (0.15 g, 0.9 mmol), pyrrole (0.15 mL, 2.1 mmol), and xylene (60 mL) as reagents, 410 mg (26%) of compound **5** was obtained after chromatography (silica gel, petroleum ether/ $CH_2Cl_2 = 1:4$ , v/v) as a purple solid, mp >250 °C.  $^1H$  NMR (500 MHz,  $CDCl_3$ )  $\delta$  9.21–9.17 (d, 4 H), 9.00 (s, 2 H), 8.88 (s, 2 H), 8.45–8.40 (m, 14 H), 8.32 (s, 8 H), 8.26–8.10 (m, 34 H), 8.03–7.95 (m, 4 H), 7.84 (s, 4 H), 7.74–7.29 (m, 116 H), –2.51 (s, 2 H, –NH). (see Figure S44, Supporting Information). MALDI-TOF: calcd 4575.6, found 4576.8 (see Figure S45, Supporting Information). Anal. Calcd for  $C_{332}H_{198}N_{28}$ : C 87.08, H 4.36, N 8.56. Found: C 87.23, H 4.40, N 8.76.

**Acknowledgment.** This work is financially supported by the National Natural Science Foundation of China (NNSFC, No. 20574027) and the Program for New Century Excellent Talents in University (NCET).

**Supporting Information Available:**  $^1H$  NMR spectra of **1–10** and **12–21**, MALDI-TOF mass spectra of **1–10**, **13**, **15**, **17**, **19**, and **21**, GPC spectra of **1–5**, UV/vis spectra of **6** recorded in different solvents, plotting between the molar extinction coefficient at 294 nm and the number of carbazoles in **6–10**, and Universal 1.02 force field optimized geometry for **1–5**. This material is available free of charge via the Internet at <http://pubs.acs.org>.

JO702426R